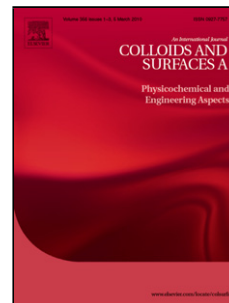# Accepted Manuscript

Title: Deposition of fluorescent NIPAM-based nanoparticles on solid surfaces: quantitative analysis and the factors affecting it

Author: Reham Mohsen Joanna B. Thorne Bruce D. Alexander Martin J. Snowden

Please cite this article as: R. Mohsen, J.B. Thorne, B.D. Alexander, M.J. Snowden, Deposition of fluorescent NIPAM-based nanoparticles on solid surfaces: quantitative analysis and the factors affecting it, *Colloids and Surfaces A: Physicochemical and Engineering Aspects* (2014), http://dx.doi.org/10.1016/j.colsurfa.2014.05.050

Deposition of fluorescent NIPAM-based nanoparticles on solid surfaces: quantitative analysis and the factors affecting it

Reham Mohsen,[a,*] Joanna B. Thorne,[a] Bruce D. Alexander[a] and Martin J. Snowden[a]

[a] School of Science, University of Greenwich, Chatham, Kent, ME4 4TB, UK

[*]Corresponding author: Reham Mohsen, e-mail: R.M.MOMEE@greenwich.ac.uk , Tel: +44 (0)20 8331 9800, Fax : +44 (0)20 8331 9805

Abstract

Recently, responsive surfaces have attracted attention due to their potential applications. Reported research have studied the deposition of environmentally responsive particles on different surfaces, qualitatively tested their response to environmental conditions and studied their possible applications. In this work, novel fluorescent temperature-sensitive nanoparticles were synthesized using a surfactant free emulsion polymerization technique: poly(*N-iso*propylacrylamide-*co*-5% vinyl cinnamate) (p(NIPAM)5%VC). The new particles were characterized using dynamic light scattering and fluorescence spectroscopy. A novel sensitive method for the quantitative analysis of p(NIPAM) 5% VC using fluorescence spectroscopy was developed to determine the concentration of nanoparticle dispersions. This was further used to quantitatively determine the mass of nanoparticles deposited per unit area of glass pre-treated with acid, glass pre-treated with base, quartz, stainless steel, gold and teflon at 25°C and 60°C. Factors affecting the adsorption/desorption of the nanoparticles were studied, including the effect of substrate surface charge, surface roughness (using atomic force microscopy, AFM), hydrophilicity/hydrophobicity and the temperature at which the adsorption/desorption experiments were carried out. The results show that the effect of surface charge is the most significant, followed by that of surface roughness and temperature. Meanwhile, the influence of the hydrophobicity/hydrophilicity of the surface on the adsorption/desorption of nanoparticles appears to be far less significant than the previously mentioned factors.

Keywords: fluorescent p(NIPAM), vinyl cinnamate, quantitative particle deposition, surface charge and surface roughness.

1. Introduction

The deposition of environmentally responsive colloidal nanoparticles on surfaces has been carried out to produce environmentally responsive surfaces. The latter can be used in many applications such as the control of cell and protein adhesion, (1-4) and bioseparation (5, 6).

For example, the reaction of stimuli-responsive surfaces with proteins can be either specific or non-specific, each of which has its own application. In the case of specific stimuli-responsive surfaces, the interactions of proteins with the surface can be controlled in order to switch the adsorption/desorption of a specific protein onto/from the surface and repel the other biological species available (7).

Alarcón *et al*. (1) managed to switch the adsorption/desorption of fluorescein isothiocyanate-labelled bovine serum albumin (FITC-BSA) on poly(*N-iso*propylacrylamide-*co*-hexadecanethiol) (p(NIPAM-*co*-HDT)) micropatterned surfaces, which was controlled by the volume phase transition temperature (VPTT) of the nanoparticles. This behaviour was less pronounced after repeated heating/cooling cycles or prolonged incubation.

1

Burkert *et al.* (2) coated silicon surfaces with a pH-thermoresponsive polymer layer of poly(2-vinyl pyridine) and p(NIPAM). This system was used to control the binding of BSA adsorption by changing the temperature from below to above the VPTT.

Qin *et al*. (3) prepared a p(NIPAM) nanoparticle with a metal chelate co-monomer *N*-(4-vinyl)-benzyl iminodiacetic acid. In the presence of Cu^{2+} ions, this co-monomer forms a co-ordination complex with the template protein. Accordingly, the addition or omission of Cu^{2+} ions can be used to switch the imprinted nanoparticle-protein interactions.

In eukaryotic cell culture, some cells can be grown in free suspension while most cells derived from solid tissues need to be cultured on a solid surface. To lift the cells off the surface, common protocols include the use of digestive enzymes such as trypsin but as a consequence it is impossible to harvest completely intact cells. Using a stimuli-responsive surface for cell culture solves this problem. Changing environmental conditions (*e.g.* temperature) at the surface changes its physicochemical properties such as surface charge and hydrophilicity; this can be used to automatically switch the cell adhesion at the surface on and off. Different physicochemical triggers were used to control cell adhesion, including electrochemistry, light and temperature (7).

Edahiro *et al*. used a photo- and thermoresponsive surface (cell culture substrate) modified with a polymerizable spiropyran derivative and a copolymer of NIPAM to switch the adhesion of Chinese hamster ovary cells on and off (8). At 37°C, when the surface was irradiated with UV light (λ=365 nm), the spiropyran was isomerized to a zwitterionic merocyanine form, which caused the cells to adhere to the surface. Reversing the isomerization by

irradiating the surface with visible light (λ=400 nm) and washing the surface with cold water caused the cells to be lifted off. Further experiments proved the viability of the cells after the UV and visible light irradiation.

Other researchers have used exclusively thermoresponsive polymers such as p(NIPAM) to coat surfaces for different applications (4). At 37°C cells tend to adhere more to hydrophobic surfaces than to hydrophilic ones. Accordingly, using the latter will provide easier removal of the cells from the surface (7).

One application of thermoresponsive polymer coatings is the separation of biomolecules. For example, silica beads modified with temperature-sensitive p(NIPAM) were used as a stationary phase for HPLC for the temperature-modulated separation of steroids and peptides.

The Okano group (5) has made progress in designing new stationary phases. In 2006, they developed a new HPLC method for the analysis of non-steroidal anti-inflammatory drugs such as ibuprofen and ketoprofen (6). They designed a new temperature/pH sensitive stationary phase by modifying aminopropyl silica beads with a NIPAM-based nanoparticle with two incorporated co-monomers: butyl methacrylate (BMA) and *N*,*N*-dimethylaminopropylacrylamide (DMAPAAm). Changing the temperature and pH caused the surface of the modified stationary phase to switch between hydrophilic/hydrophobic and charged/uncharged forms. Temperature changes can also cause the ion exchange groups to appear on the surface, which highly affects the retention time of the analytes. The authors suggest the new method will be suitable for the separation of charged biomolecules such as proteins, DNA and peptides, and they refer to this technique as 'temperature responsive chromatography'.

2

The work reported herein aims to determine the quantity of nanoparticles deposited on different surfaces under specified conditions and to discuss the factors affecting it (substrate surface charge, surface roughness, hydrophilicity/hydrophobicity and the temperature at which the deposition/desorption processes take place. This is important to move the applications of stimuli responsive surfaces from the research phase to the practical application one with special consideration to the commercial factors associated with this process. To determine the amount of nanoparticles deposited on a surface, a simple dip-coating technique was used, where the solid surface was dipped into a nanoparticle dispersion of known loading, then left for three hours before the concentration of the supernatant was measured to infer the number of nanoparticles deposited on the surface. A new fluorescent-labelled nanoparticle was synthesized and fluorescence spectroscopy was used to determine the concentration of the nanoparticles in the dispersions before and after solid dipping. This increases the sensitivity and reliability of the quantitation of deposited particles.

2. Materials and methods
2.1 Nanoparticle synthesis

In a 1 L reaction vessel, 1.84 mM of the initiator 2,2-azobis(2-methylpropionamidine was dissolved in 800 mL of distilled water. A three-necked lid was clamped to the reaction vessel, which was then heated to 70°C with continuous stirring. The monomer (41.97 mM NIPAM), co-monomer (1.43 mM vinyl cinnamate, VC) and cross linker (3.24 mM *N,N*'-methylenebisacrylamide) were stirred in distilled water (200 ml) then transferred into the reaction vessel containing the initiator and continuously stirred at 70°C for six hours under an inert atmosphere of nitrogen. When the reaction was complete, the nanoparticle dispersion

was allowed to cool to room temperature. Given the photosensitivity of fluorescent VC, all the glassware used was wrapped in aluminium foil to protect the reaction from light and avoid the dimerization of VC molecules, which may have interfered with the polymerization reaction. The nanoparticle dispersion was dialyzed in fresh de-ionised water changed daily for a week, centrifuged and freeze dried. The resulting novel poly(NIPAM-*co*-5% vinyl cinnamate) nanoparticles are herein referred to as p(NIPAM)5%VC .

A 100% p(NIPAM) dispersion was also prepared using the same method (without incorporation of the VC co-monomer), so that the characteristics of the novel p(NIPAM)5%VC co-polymer particles could be compared with those of a standard, well characterised system.

2.2 Nanoparticle characterization

2.2.1 Dynamic light scattering
Dynamic light scattering (DLS) measurements were carried out using a Malvern Zetasizer Nano ZS and a quartz cuvette with two polished windows (Starna Type 1). All samples were diluted with deionized water (1 mL of dialysed nanoparticle dispersion was diluted with 2 mL of water) before measurements. The hydrodynamic diameter of the particles was measured in response to temperature change from 15 to 60°C). The temperature of the dispersion was controlled by a Peltier thermocouple. Data were collected every 1°C and the samples were equilibrated for 2 min before each data collection point. Three measurements, each consisting of 13 subruns, were taken at each temperature to obtain an average hydrodynamic diameter. The pH of the samples was adjusted to pH 3 and 10 using diluted HCl and NaOH to test for the effect of changing pH upon the size of the particles.

3

2.2.2 Fluorescence spectroscopy

A Horiba Jobin Yvon Fluoromax 4 spectrofluorometer was used for fluorescence experiments to determine the mass of nanoparticles either deposited or subsequently desorbed from each surface. Firstly, a calibration curve was obtained using a known concentration of p(NIPAM)5%VC dispersion that was prepared by re-dispersing freeze dried particles in water then underwent serial dilution. All samples were excited at 300 nm and the full emission spectra (315-540 nm) were recorded with bandwidth of 5 nm at 25°C. A 10 mm path length quartz cuvette with four polished windows (Starna Type 3) was used for all the measurements.

2.3 Slide surface treatments

2.3.1 Glass and quartz

Glass microscope slides were supplied by Sail Brand (75 x 25 mm, 1–1.2 mm thick). Quartz microscope slides (75 x 25 mm) were supplied by GPE Scientific Limited. To study the effect of surface treatment on the mass of nanoparticles adsorbed on the surface, two types of glass surface were tested.

The acid pre-treated glass and quartz slides were prepared in the same way: they were thoroughly washed with de-ionized water, sonicated in MeOH:HCl (1:1) (pH 0.12) for 30 min, thoroughly washed with de-ionized water, sonicated in 2M H_2SO_4 for 30 min then finally rinsed with de-ionized water and stored in MeOH. The base pre-treated glass slides were thoroughly washed with de-ionized water, sonicated in MeOH:NaOH (pH 11) for 30 min, rinsed with deionised water and stored in MeOH. Prior to use, all the slides were thoroughly washed with water and dried under N_2.

2.3.2 Stainless steel

Stainless steel slides were supplied by Reco Engineering Components Limited (75 x 25 mm, 1.2 mm thick). The slides were physically cleaned with wire wool, sonicated in 1.5% NaOH (pH 11) for an hour and then dried in oven at 50°C for an hour before use.

2.3.3 Gold

Clean microscope glass slides were coated with pure gold obtained from Agar Scientific by sputter coating from an Edwards 150B sputter coater. Both sides of the glass slides were coated before being kept in a clean container and used without any further treatment.

2.3.4 Teflon

A PTFE plastic sheet stock was supplied by RS Company and laser cut into slides (75 x 25 mm). The slides were thoroughly washed and sonicated for an hour in fresh soapy water (Teepol multipurpose detergent), then stored in fresh soapy water. Prior to use slides were thoroughly washed with de-ionized water and dried under N_2.

2.4 Surface deposition/desorption of nanoparticles

2.4.1 Deposition

Dip coating was used to deposit nanoparticles onto the different slide surfaces. The solid slides were dipped into Petri dishes containing 20 mL of a 2% w/v dispersion of p(NIPAM)5%VC. For each type of solid surface, three samples were coated (deposited) at 25°C and three at 60°C. Control experiments (of nanoparticle dispersion alone, with no dipping of slides) were conducted in parallel to account for the adsorption of nanoparticles on petridishes.

The slides were left covered in the Petri dishes for 3 hours. The slides were then removed from the residual nanoparticle dispersions, which were then analysed using fluorescence spectroscopy (Section 2.5.1).

4

2.4.2 Desorption

For desorption experiments, the solid slides previously used in the deposition experiments (Section 2.4.1) were dipped in Petri dishes containing 20 mL of deionized water and left for 3 hours. Again for each type of solid surface, three samples were desorbed at 25°C and three were desorbed at 60°C. Parallel control experiments were carried out to account for the deposition of nanoparticles on petridishes. The residual nanoparticle dispersions were then analysed using fluorescence spectroscopy (Section 2.5.1).

2.5 Surface characterization

2.5.1 Fluorescence spectroscopy

For the fluorescence measurements in all the deposition experiments, as well as the glass, quartz and stainless steel desorption experiments, the residual nanoparticle dispersions remaining after deposition/desorption were firstly stirred then diluted by a factor of 1/4000. For the gold and teflon desorption experiment fluorescent measurements, the residual nanoparticle dispersions remaining after desorption were stirred but used undiluted. Measurements were carried out the same way as section 2.2.2.

The concentration of nanoparticles (w/v) in the residual dispersions was calculated from the fluorescence intensity measurements using the calibration curve (Figure 3), then the mass of nanoparticles in each residual dispersion was determined. The mass of nanoparticles deposited was calculated by subtracting the mass of nanoparticles in the residual dispersion from that in the control (2 % w/v nanogel dispersion in a petridish that is treated the same as the sample).

2.5.2 AFM

A Nanosurf easyscan 2 AFM was used to analyse both bare surfaces and surfaces with deposited nanoparticles. Tapping mode was used using Tap190Al-G tips supplied by Budget Sensors. The image size per run was 10µm at a resolution of 1024 lines, each containing 1024 points. The time per line was 1.5s. Three sites per slide and three slides of each sample were tested to look at the uniformity of results.

3. Results and discussion

Cinnamic acid derivatives are widely used as fluorescent probes (9). They also possess some biological activity including an anti-tumor effect (9, 10). In this work, VC was used as a co-monomer to synthesize fluorescent colloidal nanoparticles. The presence of a pendant vinyl group in the molecular structure of VC makes it readily polymerizable.

3.1 Characterization of p(NIPAM)5%VC nanoparticles
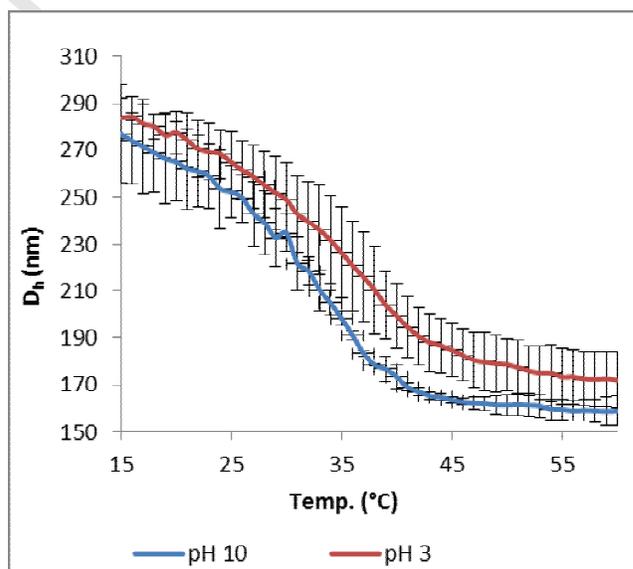
3.1.1 Size and VPTT

Figure 1 shows the change in particle size of p(NIPAM)5%VC in response to temperature change. The initial particle diameter (below the VPTT) is approximately 280 nm and shrinks to 160

5

nm upon increasing the temperature above the VPTT. This is significantly smaller than 100% p(NIPAM) (synthesized in the same way) with a typical initial particle size of 550 nm (11) that shrinks to 290 nm above the VPTT. The incorporated hydrophobic VC decreases the extent of hydrogen bonding between the particle and water compared to 100% p(NIPAM), so less water will be incorporated in the particle, leading to a smaller particle size.

Figure 1 also indicated that the VPTT of the p(NIPAM)5%VC nanoparticles is around 32-35°C, very similar to the VPTT of 34°C reported for the p(NIPAM) nanoparticles (11). Together, these results confirm that incorporation of VC did not lead to a loss of thermosensitivity of the nanoparticles but did influence (reduce) the nanoparticle size and extent of de-swelling.

Figure 1 also shows no significant difference between the particle size at pH 3 and 10. This is because the VC molecule does not include ionizable groups that would be affected by the change in pH. The minimal difference observed between the two pHs can be attributed to the cationic initiator groups on the particle surface.

3.1.2 Fluorescence spectroscopy

In order to confirm whether the VC co-monomer had been incorporated into the nanoparticle structures, the emission spectra of 100% p(NIPAM) was compared with that of p(NIPAM)5%VC when excited at the same wavelength (300 nm) (Figure 2). There is a clear shift in the emission band when comparing the two spectra. Furthermore, the p(NIPAM)5%VC has the same reported λ_{em} as that of VC (350 nm) (12), which also supports the conclusion that VC was incorporated into the new particles.
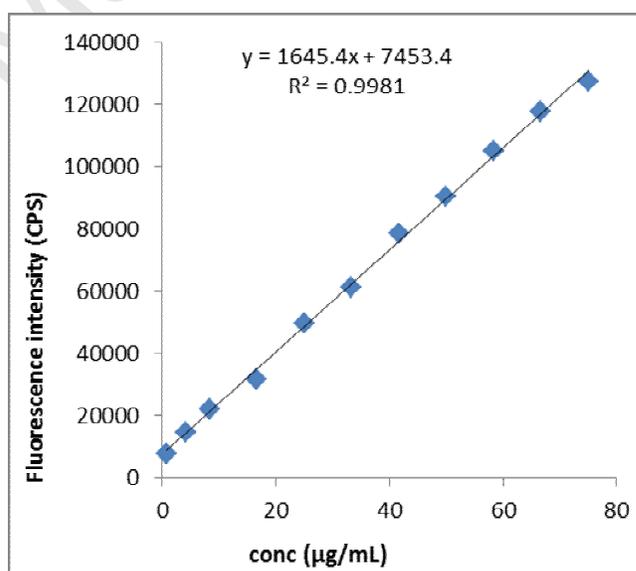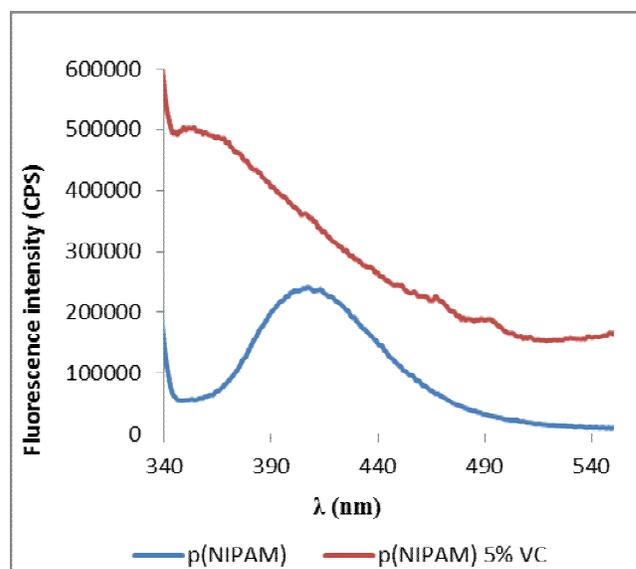
In order to determine the concentration (w/v) of dispersions containing an unknown quantity of p(NIPAM)5%VC, a calibration curve at 25°C was prepared (Figure 3).
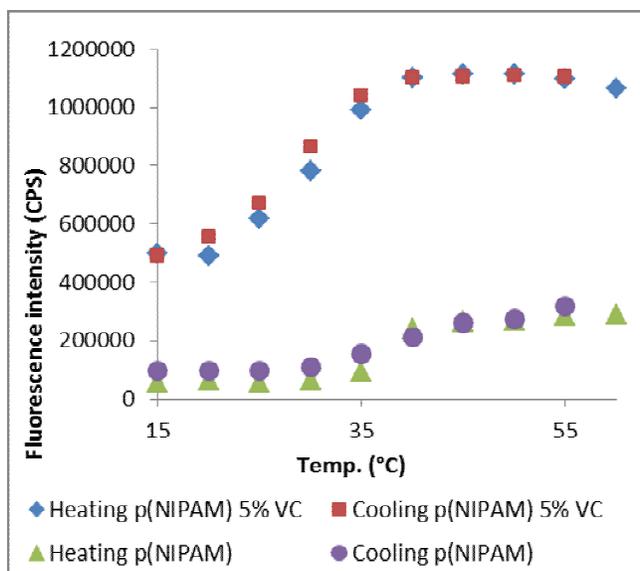
6

Figure 4 compares the response of 50 μg/mL p(NIPAM)5%VC and 100% p(NIPAM) to changing temperature (heating-cooling) using fluorescence spectroscopy. When the temperature increases, the temperature-sensitive nanoparticles shrink. This increases the local density of the incorporated VC fluorophores within the particle, leading to an increase in the overall fluorescence intensity of the nanoparticle dispersion.

Figure 4 shows that the fluorescence intensity of p(NIPAM)5%VC is almost five times greater than that of 100% p(NIPAM) considering that both dispersions are of the same concentration. Therefore, addition of a VC fluorophore co-monomer provides a sensitive method for the quantitative analysis of the concentration (w/v) of nanoparticle dispersions.

3.2 Factors affecting the mass of p(NIPAM) 5% VC deposited on different surfaces
Table 1 shows the mass of nanoparticles adsorbed on each surface based on fluorescence spectroscopy measurements.

At 25°C (lower than the VPTT of p(NIPAM) 5% VC, Figure 1). Stainless steel adsorbed the highest mass of nanoparticles followed by glass pre-treated with base, glass pre-treated with acid, quartz, gold then teflon. The mass of nanoparticles deposited on steel was about five times that deposited on glass, ten times that deposited on quartz, fifty of gold and three hundred and sixty that on teflon.

Not only did steel have a large mass of nanoparticles deposited on its surface but also a low desorption percentage and therefore the highest affinity towards the nanoparticles.

At 60°C (above the VPTT of p(NIPAM)5% VC) the mass of particles deposited on all surfaces was increased and, apart from base pre-treated glass, the percentage desorption decreased. The factors affecting the net mass of nanoparticles deposited on or desorbed from the different surfaces will be discussed in detail.

3.2.1 Effect of surface charge
For any given solid surface, usually there are functional groups expressed on the surface. The extent of ionization of these groups can be altered by changing the pH of the surrounding environment. This can be used to control the adsorption/desorption onto/from a solid surface. Therefore slide surface charge can be described by the point of zero charge (PZC). This is the pH where the net charge on the surface is zero (13).

Stainless steel
Takehara and Fukuzaki (14) reported the importance of stainless steel treatment on controlling its surface charge. They compared the surface charge of non-treated and acid-treated stainless steel and claimed that the surface charge is affected

7

Table 1: Expected and measured characteristics of slide surfaces before deposition of nanoparticles (surface charge, relative hydrophobicity and surface roughness), and nanoparticle mass deposited and % desorbed from slide surfaces at 25 and 60 °C

Slide surface	Expected slide surface charge[1]	Contact angle and hydrophobicity/ hydrophilicity	Measured S_a (nm)	25°C		60°C	
				Net mass nanoparticles deposited (mg/m^2)	% desorption	Net mass nanoparticles deposited (mg/m^2)	% desorption
Stainless steel	Negative	70-75° Hydrophobic (15)	89.6	21.64 (3.87)	6.30	25.84 (1.10)	4.20
Gold	Negative	56-66° Hydrophobic (15, 16)	7.07	0.43 (0.02)	41.00	5.32 (2.88)	6.60
Quartz	Slightly negative	22° Hydrophilic (17)	0.37	1.99 (1.60)	55.70	2.91 (2.22)	39.00
Base pre-treated glass	Negative	<10° Hydrophilic (17)	0.02	4.83 (1.38)	0.06	8.94 (0.80)	19.00
Acid pre-treated glass	Slightly negative		0.02	3.71 (0.85)	2.87	4.55 (1.89)	0.20
Telfon	Neutral	102° Hydrophobic (17)	103.7	0.06 (0.03)	90.00	2.13 (1.15)	34.00

[1] Expected slide surface charge at pH of deposition nanoparticle dispersion (pH 6.7)
[2] Standard deviations presented in brackets

8

by the protonation ($M\text{-}OH_2^+$) and hydroxyl groups. Accordingly, acid treated stainless steel exhibited a protonated positive charge.

Tanaka *et al.* (18) studied the concentration of hydroxyl groups on stainless steel surfaces and determined the PZC. The EDX data (in the supplementary data) show a similarity between the composition of stainless steel used in this work and that used by Tanaka, who found untreated stainless steel to have a PZC of 5.6. Accordingly, it was claimed that the surface charge of stainless steel in a solution of pH 11 (far above the PZC) is negative.

In this work, stainless steel samples were sonicated in NaOH (pH 11) to expose the surfaces to a pH far above the PZC to ensure that the surface charge of the slides was negative prior to immersion in the nanoparticle dispersion. Also, knowing that the pH of the nanoparticle dispersion used for adsorption experiments carried out in this work is 6.7 (still above the PZC of stainless steel), it can be concluded that the surface charge of stainless steel immersed in the nanoparticle dispersion remains negative.

The negatively charged stainless steel surface electrostatically attracts the positively charged nanoparticles (which are cationic due to the initiator used during the particle synthesis). This increases the mass of nanoparticles deposited on the surface as well as decreases the percentage desorption and hence stainless steel showed a high net deposited mass of nanoparticles (Table 1).

Glass and quartz

When immersed in a liquid, the surface charge of glass depends on its chemical composition and the pH of the solution. This can either cause the association or dissociation of protons to/from the oxide surface leading to positive or negative

deprotonation ($M\text{-}O^-$) of the surface surface charge, respectively (Equations 1a and b) (19, 20).

$$SiOH + H^+ \rightleftharpoons SiOH_2^+ \quad (a)$$

$$SiOH \rightleftharpoons SiO^- + H^+ \quad (b)$$
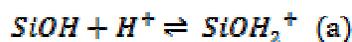
Equation 1: Protonation/deprotonation of silicon hydroxide in (a) acidic and (b) alkaline media

The point of zero charge of glass is pH 3.5, while that of silica is pH 2.8 (21). In this work, glass slides pre-treated with acid and base were used, whilst quartz samples were treated with acid.

For the base pre-treated glass samples, the pH of the solution used for sonication was much higher than the PZC of glass. So, the glass slide surface charge at this point was considered to be strongly negative. When immersed in the nanoparticle dispersion with a pH above the PZC, the glass surface charge is still expected to be strongly negative.

For the acid pre-treated samples (glass and quartz), the pH of the solutions used for treatment was much lower than the PZC of both glass and quartz, so, the surface charge of the treated sample surfaces was considered to be positive, with $SiOH_2^+$ groups dominant on the surface prior to immersion in the nanoparticle dispersion. When immersed in the nanoparticle dispersion with pH (6.7) above the PZC of both glass and quartz, surfaces are expected acquire a low magnitude of negative charge. In comparison to the base pre-treated glass samples, both glass and quartz pre-treated with acid are expected to have relatively fewer negative charges on their surface.

Table 1 shows that the mass of nanoparticles deposited on glass samples pre-treated with a base (highly negatively charged) was more than that deposited on

9

those pre-treated with acid (with relatively less negative surface charge than the base treated slides). Also, the percentage of desorption of particles from base-treated glass samples was much less than that of the acid-treated ones at 25 °C. This is attributed to the strong electrostatic attraction between the highly negatively charged surface (base pre-treated samples) and the positively charged particles; these forces are much less for the acid pre-treated slides and hence the much higher percentage desorption. This indicates that the effect of substrate surface charge on the mass of deposited particles is pronounced.

At 60°C, the same pattern of results is observed except that the percentage desorption of particles from the base treated glass is higher than that desorbed from the acid treated one (Table 1). This could be due to increased repulsion forces between the positively charged particles (which have an increase in surface charge density when the temperature exceeds the VPTT (22).

Gold

Barten *et al*. (23) studied the deposition of linear positively charged poly-2-vinyl pyridine (PVP$^+$) on a gold electrode. Knowing that the PZC of gold is 4.9 (23), they studied the effect of changing the pH in the range of 3.5 to 6 (it is claimed that the surface charge of gold is constant above pH 6) (23). A slight increase in the adsorbed amount of PVP$^+$ upon increasing the pH of the solution was reported. This can be attributed to the increase of the electrostatic attraction forces between the negatively charged surface (gold in pH above 4.9) and the positively charged PVP$^+$.

In this work, gold-coated glass was immersed in a nanoparticle dispersion of pH 6.7. Being above the PZC of gold (4.9) (23), the surface was then expected to be negatively charged. This suggests the presence of electrostatic attraction forces between the negatively charged substrate surface and the positively charged particles which is expected to result in a high net deposition mass of nanoparticles. However, table 1 shows that the mass of nanoparticles deposited on gold substrate surfaces is the second lowest deposited mass when compared to the other surfaces. This can be attributed to the magnitude of negative charge on each substrate surface.

Teflon

The molecular structure of teflon is a polymer of tetrafluoroethene. The absence of ionisable groups in the polymer suggests that the surface is neutral. For this reason, teflon surfaces are said to have low surface energy and hence used as non-stick materials. So, the effect of the substrate surface charge is expected to be eliminated in this case. This is reflected by the fact that the mass of nanoparticles deposited on teflon was observed to be the least compared to the other substrates.

The expected surface charge of each surface and their relative hydrophobicities are summarized in Table 1. An electrostatic attraction force is generated between the negatively charged surfaces (stainless steel, base pre-treated glass, acid pre-treated glass, quartz and gold) and the positively charged nanoparticles. For the acid pre-treated glass and quartz samples, the electrostatic attraction force between the surface and the particle is expected to be less than that between the base pre-treated glass sample and the particle. On the other hand, teflon is neutral and thus there is no electrostatic force in this case.

Table 1 shows that the highest mass of deposited nanoparticles and the lowest desorption percentages were observed for stainless steel, base pre-treated glass, acid pre-treated glass, quartz and gold (negatively charged surfaces), while the neutral surface (teflon) had the lowest deposition mass and the highest desorption

10

percentage. Accordingly, the data suggest that the surface charge affects the mass of nanoparticles adsorbed on/desorbed from surfaces. The magnitude of the slide surface charge is also thought to be a significant factor affecting the adsorption/desorption of nanoparticles on/from different negative surfaces. It was not possible to measure this within the scope of this study, however, as per discussed, an estimate of the relative surface charge could be inferred (e.g. acid pre-treated glass was relatively less negatively charged than the base pre-treated one).

For the same surface (glass), increasing the negative surface charge on the glass slide by treating it with a base rather an acid increases the electrostatic attraction force between the negative glass surface and the positive nanoparticle which increases the mass of deposited nanoparticles (Table 1).

At 60°C, the ranking of different solid surfaces considering the adsorption / desorption of nanoparticles on/from the surface is similar to that at 25°C. The minor changes observed (for example, at 25°C the mass of nanoparticles adsorbed on acid pre-treated glass is more than that adsorbed on quartz while at 60°C, the opposite is observed) are thought to be due to the increased particle surface charge at 60°C (above the VPTT) which increases the electrostatic repulsion between particles. Also, the difference between the magnitude of surface charge of the different solid slide substrates will be an important factor.
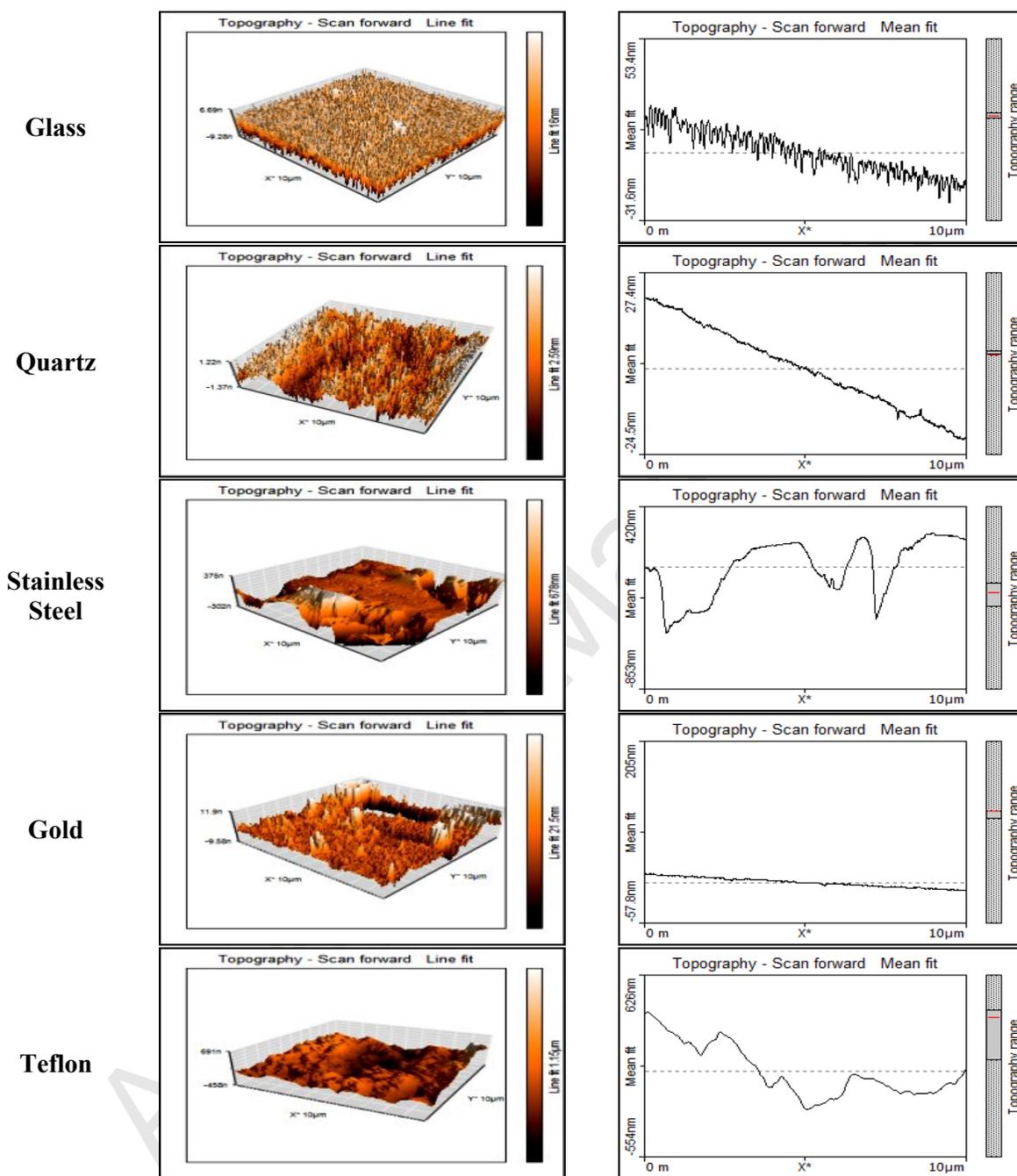
3.2.2 Effect of surface roughness
Surface roughness is a description of the 'irregularity' of a surface (24). Figure 5 and Table 1 provide AFM topography images of each surface and the roughness average (S_a) of different surfaces before the deposition of nanoparticles. These can be determined from line profiles across a section of surface (Equation 2).

$$S_a = \frac{1}{L} \int_0^L |z(x)| dx$$

**Equation 2: Calculation of average surface roughness**

Where L is the evaluation length, z is the height and x is the distance along measurement.

S_a is the area between the roughness profile and its mean line (Equation 2) (24). The higher the S_a value, the deeper and/or wider are the pores on the sample surface. These pores can trap nanoparticles inside and increase the surface area where the particles can be adsorbed. The S_a values of the solid surfaces before the deposition of nanoparticles (Table 1) show that Teflon has the highest surface roughness used in this work, followed by stainless steel, gold, quartz and glass respectively. Comparing the surface roughness data (Table 1 and Figure 6) to that of deposition (Table 1), one can conclude that the degree of irregularity of the surface does not affect the mass of nanoparticles deposited on/desorbed from it. For example, at 25 °C, Teflon had the highest S_a and yet it had the lowest adsorption and the highest desorption percentage, whilst stainless steel had the second highest S_a, the highest deposition but one of the lowest desorption values. On the other hand, correlating the effect of surface roughness with that of surface charge, it is clear that for negatively charged surfaces (stainless steel gold, quartz and base-treated glass), the one that the possess a significantly higher S_a (stainless steel) showed higher adsorption and lower desorption than the rest. For the latter three negatively charged surfaces where there was not much difference in S_a, the magnitude of surface charge is thought to be the main reason why the mass of nanoparticles adsorbed

11

Glass

Quartz

Stainless Steel

Gold

Teflon

12
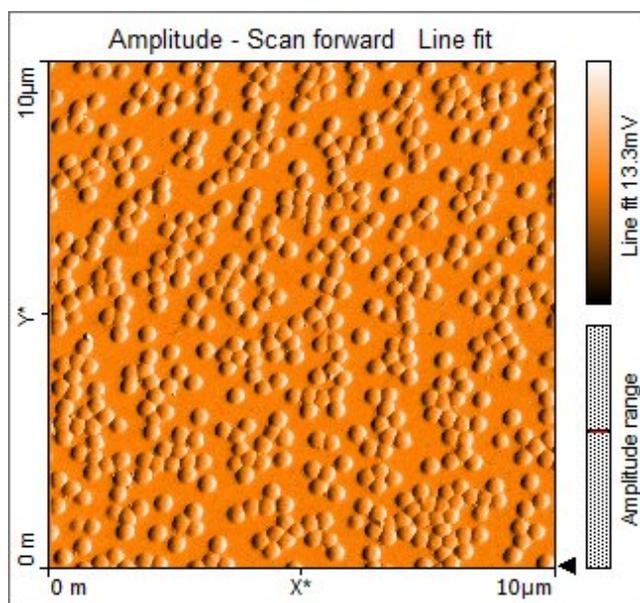
(a)
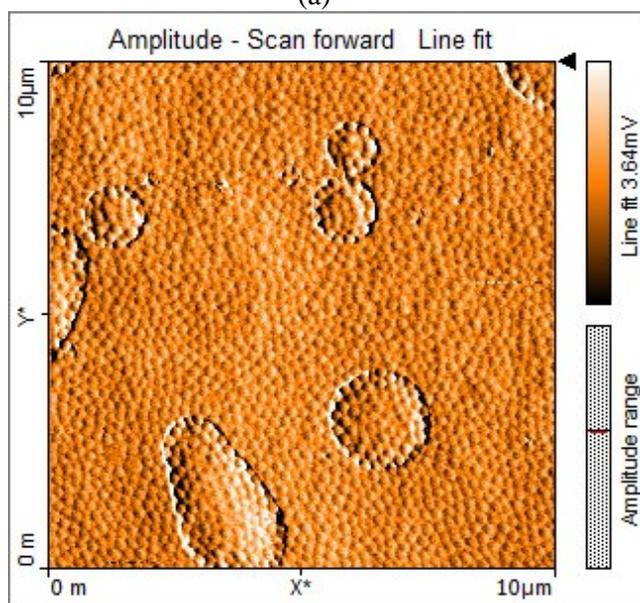
(b)

Figure 6: AFM images of p(NIPAM)5%VC particles deposited on glass (a) at 25˚C and (b) at 60˚C

on/desorbed from the surface varied. Hence, it can be concluded that the surface roughness can be considered as a secondary effect that boosts that of surface charge. The combination of both (surface charge and roughness) strongly influences the extent of adsorption and desorption on/from the surface.

Comparing the mass of the net adsorbed particles on the stainless steel and base-treated glass samples (Table 1) supports this explanation. Both samples acquire a negative surface charge, yet the adsorption of the positive nanoparticles on the stainless steel surface is 4.5 times more than that on glass. This is thought to be due to the fact that the average surface roughness of stainless steel is significantly higher than that of glass (Table 1 and Figure 5).

3.2.3   Effect   of   hydrophilicity/ hydrophobicity

The comparison of the hydrophilicity/ hydrophobicity of all surfaces (Table 1) suggests that this factor has minimal effect on the amount of particles deposited on/desorbed from different surfaces. The surface with the highest adsorption and lowest desorption percentage (stainless steel) and that with the lowest adsorption and highest desorption (teflon) are both thought to be hydrophobic (15, 17). Also, the difference between the mass of particles deposited on hydrophilic surfaces is significant. This suggests that the effect of hydrophilicity/hydrophobicity is of less importance than that of substrate surface charge and surface roughness. However, further studies with more systematic comparison characters may help elucidate influence of relative hydrophilicity in more details.

3.2.4 Effect of temperature

The deposition/desorption data provided in table 1 shows that the mass of nanoparticles deposited on all surfaces at 60°C was higher than that at 25°C. Also, the percentage desorption decreased with temperature (except for base pre-treated glass), leading to an increased net mass of deposition. When the temperature increases above the VPTT (32°C), the particles deswell (Figure 4). This means that the surface charge density on the particle increases which increases the electrostatic attraction between the positively charged nanoparticles and the negatively charged surfaces. Also, the

13

number of de-swollen particles that fit in the pores of solid surfaces will be more than that of the swollen ones. AFM images (Figure 6) show that increasing the temperature above the VPTT affects the packing of the particles. In case of base pre-treated glass, the percentage of desorbed nanoparticles is more than that at 25°C. The suggested reason for this is the increased electrostatic repulsion between the positive nanoparticles when the temperature exceeds the VPTT (32°C).

Table 2: Comparison between the surface roughness averages of glass, quartz, stainless steel, gold and teflon coated with p(NIPAM)5%VC nanoparticles at 25°C and 60°C

	S_a at 25°C (nm)	S_a at 60°C (nm)
Stainless steel	65	77
Gold	10	9
Quartz	25	10
Glass pre-treated with base	17	9
Glass pre-treated with acid	18	10
Teflon	19	43

Table 2 shows the S_a of adsorbed particles on different surfaces at 25 and 60°C. Despite the fact that the mass of nanoparticles deposited at 60°C is higher than that deposited at 25°C (Table 1), the S_a (representing the roughness of the deposited layer) is generally (except for stainless steel and teflon) smaller at 60°C than at 25°C. This is due to the regular dense packing of particles at 60°C while at 25°C this is not always the case (Figure 6). In case of stainless steel and teflon, the S_a at 60°C is bigger than that at 25°C. This is thought to be caused by the increased electrostatic repulsion force between the positive nanoparticles (due to increased surface charge density above the VPTT).

4. Conclusion

A novel fluorescent temperature sensitive nanoparticle (p(NIPAM)5%VC) was synthesized and characterized. It was then used to develop a novel sensitive method (using fluorescence spectroscopy) to quantify the mass of nanoparticles deposited on different solid surfaces per unit area and the factors affecting it. The mass of nanoparticles deposited on/desorbed from different surfaces is affected by different factors, the most important of which is the surface charge followed by the surface roughness of the solid surface. The effect of temperature has also proved to be significant since it alters the physico-chemical properties of the nanoparticles and hence alters its interaction with the solid surface. On the other hand, the effect of hydrophilicity / hydrophobicity of the solid surface was shown to be of less importance than the previously tested factors.

5. References

1. C. Alarco, T Farhan, V. Osborne, W. Huckb and C. Alexander. Bioadhesion at micro-patterned stimuli-responsive polymer brushes. Journal of Materials Chemistry. 2005:15:2089–94.
2. S. Burkert E. Bittrich, M. Kuntzsch, M. Muller, K. Eichhorn, C. Bellmann, P. Uhlmann and M. Stamm. Protein Resistance of PNIPAAm Brushes: Application to Switchable Protein Adsorption. Langmuir. 2010:26:1786–95.
3. L. Qin, X. He, W. Zhang, W. Li and Y. Zhang. Macroporous thermosensitive imprinted hydrogel for recognition of protein by metal coordinate interaction. Anal Chem. 2009:81:7206–16.
4. K. Nagase, J. Kobayashi, and T. Okano. Temperature-responsive intelligent interfaces for biomolecular separation and cell sheet engineering. J R Soc Interface. 2009:6:S293–S309.
5. H. Kanazawa, M. Nishikawa, A. Mizutani, C. Sakamoto, Y. Morita-Murase, Y. Nagata, A. Kikuchi and T. Okano.

14

Aqueous chromatographic system for separation of biomolecules using thermoresponsive polymer modified stationary phase. Journal of Chromatography A. 2008;1191:157-61.

6. E. Ayano, K. Nambu, C. Sakamoto, H. Kanazawa, A. Kikuchi, T. Okano. Aqueous chromatography system using pH- and temperature-responsive stationary phase with ion-exchange groups. Journal of Chromatography A. 2006:1119:58-65.

7. E. Wischerhoff, N Badi, A. Laschewsky and J. Lutz. Smart polymer surfaces: concepts and applications in biosciences. Advanced Polymer Science. 2011:240:1-33.

8. J. Edahiro, K. Sumaru, Y. Tada, K. Ohi, T. Takagi, M. Kameda, T. Shinbo, T. Kanamori and Y. Yoshimi. In situ control of cell adhesion using photoresponsive culture surface. Biomacromolecules. 2005: 6:970-4.

9. T. Singh and S. Mitra. Interaction of cinnamic acid derivatives with serum albumins: A fluorescence spectroscopic study. Spectrochimica Acta Part A: Molecular and Biomolecular Spectroscopy. 2011:78:942–8.

10. J. Min, X. Meng-Xia, Z. Dong, L. Yuan, L. Xiao-Yu and C. Xing. Spectroscopic studies on the interaction of cinnamic acid and its hydroxyl derivatives with human serum albumin. Journal of Molecular Structure. 2004:692:71–80.

11. R. Mohsen, G. Vine, N. Majcen, B. Alexander and M. Snowden. Characterization of thermo and pH responsive NIPAM based microgels and their membrane blocking potential. Colloids and Surfaces A: Physicochemical and Engineering Aspects. 2013:428:53-9.

12. J. Torres. Designing dual thermoresponsive & photoresponsive materials for biomedical applications: McMaster University: 2011.

13. C.Appel, L. Ma, R. Rhue, E. Kennelley. Point of zero charge determination in soils and minerals via traditional methods and detection of electroacoustic mobility. Geoderma. 2003:113:77– 93.

14. A. Takehara and S. Fukuzaki. Effect of the Surface Charge of Stainless Steel on Adsorption Behavior of Pectin Biocontrol Science. 2002:7:9-15.

15. B. Arkles. Hydrophobicity, Hydrophilicity and Silanes. Paint & Coatings Industry magazine. 2006.

16. K. Osborne. Temperature-Dependence of the Contact Angle of Water on Graphite, Silicon, and Gold. Worcester Worcester Polytechnic Institute: 2009.

17. A. Sumner E. Menke, Y. Dubowski, J. Newberg, T. Brauners, B. Finlayson-Pitts. The nature of water on surfaces of laboratory systems and implications for heterogeneous chemistry in the troposphere. Phys Chem Chem Phys. 2004:6:604–613.

18. Y. Tanaka, H. Saito, Y. Tsutsumi, H. Doi, H. Imai and T. Hanawa. Active Hydroxyl Groups on Surface Oxide Film of Titanium, 316L Stainless Steel, and Cobalt-Chromium-Molybdenum Alloy and Its Effect on the Immobilization of Poly(Ethylene Glycol). Materials Transactions. 2008:49:805-11.

19. R. Sabia and L. Ukrainczyk. Surface chemistry of SiO_2 and $TiO_2\pm SiO_2$ glasses as determined by titration of soot particles. Journal of Non-Crystalline Solids. 2000:277:1-9.

20. S. Behrens and D. Grier. The Charge of Glass and Silica Surfaces. 2008.

21. H. Churchill, H. Teng and R. Hazen. Correlation of pH-dependent surface interaction forces to amino acid adsorption: implications for the origin of life. American Mineralogist. 2004:89:1048–55.

22. J. Thorne, G. Vine, M. Snowden. Microgel applications and commercial considerations. Colloid Polym Sci. 2011: 289:629-646.

23. D. Barten, J. Kleijn and M Cohen Stuart. Adsorption of a linear polyelectrolyte on a gold electrode. Phys Chem Chem Phys. 2003:5:4258–64.
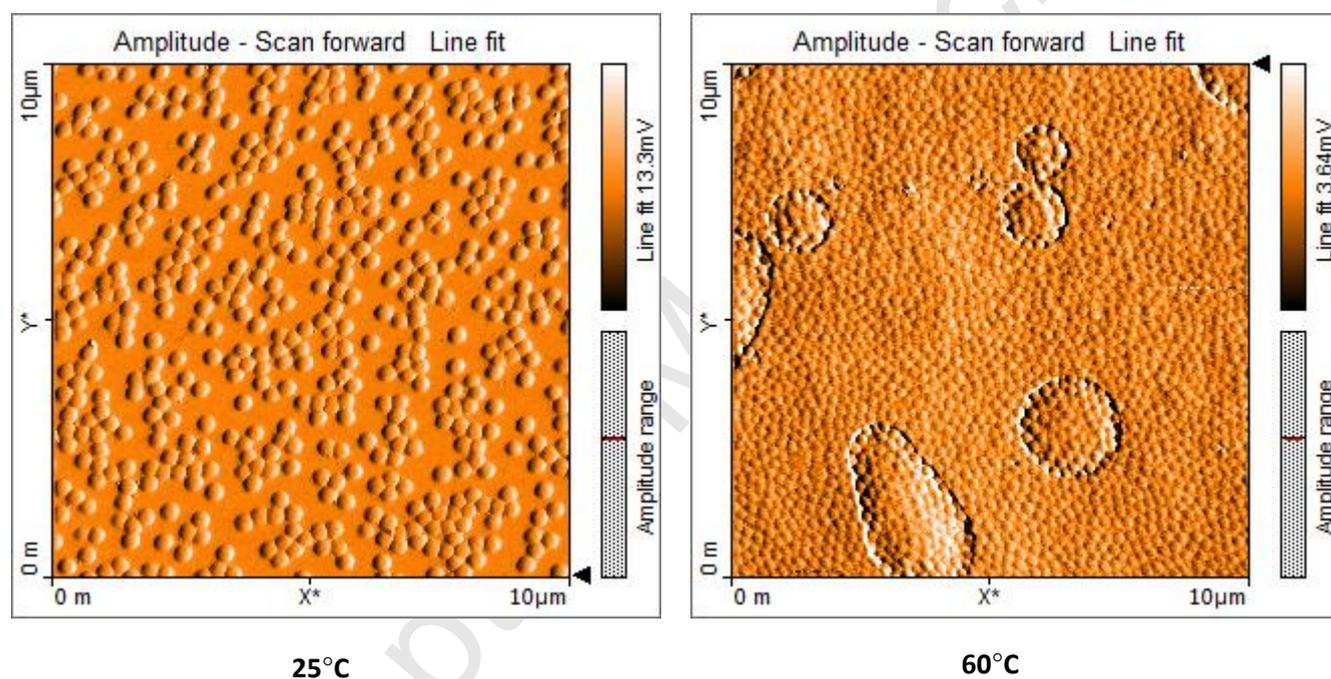
24. R. Amaral and L. Chong. Surface Roughness, 2002.

15

Deposition of fluorescent NIPAM-based nanoparticles on solid surfaces: quantitative analysis and the factors affecting it

Reham Mohsen,[a,*] Joanna B. Thorne,[a] Bruce D. Alexander[a] and Martin J. Snowden[a]

[a] School of Science, University of Greenwich, Chatham, Kent, ME4 4TB, UK

[*]Corresponding author: Reham Mohsen, e-mail: R.M.MOMEE@greenwich.ac.uk , Tel: +44 (0)20 8331 9800, Fax : +44 (0)20 8331 9805

Graphical abstract

25°C   60°C

Deposition of fluorescent NIPAM-based nanoparticles on solid surfaces: quantitative analysis and the factors affecting it

Reham Mohsen,[a,*] Joanna B. Thorne,[a] Bruce D. Alexander[a] and Martin J. Snowden[a]

[a] School of Science, University of Greenwich, Chatham, Kent, ME4 4TB, UK

[*]Corresponding author: Reham Mohsen, e-mail: R.M.MOMEE@greenwich.ac.uk , Tel: +44 (0)20 8331 9800, Fax : +44 (0)20 8331 9805

Highlights:

1- A novel fluorescent temperature-sensitive nanoparticle, p(NIPAM) 5% VC, was synthesized.

2- Quantitative analysis of the deposition of nanoparticles on different surfaces was carried out.

3- A combination of factors affects the mass of nanoparticles deposited on surfaces.

4- Surface charge, surface roughness and temperature highly affect the mass of nanoparticles deposited on different surfaces.

5- The hydrophilicity/hydrophobicity of the surface has minimal effect on the deposition of nanoparticles.